LBL-25464
Preprint

Lawrence Berkeley Laboratory
UNIVERSITY OF CALIFORNIA

Submitted to Physics Letters B

Production of Helium (Z=2) Projectile Fragments in ^{16}O Interactions at 200*A* GeV

EMU-01 Collaboration

May 1988

Prepared for the U.S. Department of Energy under Contract Number DE-AC03-76SF00098.

Production of Helium (Z=2) Projectile Fragments in ^{16}O Interactions at 200A GeV

EMU-01 Collaboration

M.I. Adamovich,[a] Y.A.Alexandrov,[a] S.A. Asimov,[b] S.K. Badyal,[c] E. Basova,[d] K.B. Bhalla,[e] A. Bhasin,[c] R.A. Bondarenkov,[d] T.H. Burnett,[f] X. Cai,[g] L.P. Chernova,[b] M.M. Chernyavsky,[a] B. Dressel,[h] E.M. Friedlander,[i] S.I. Gadzhieva,[b] E.R. Ganssauge,[h] S. Garpman,[j] S.G. Gerassimov,[a] A. Gill,[e] J. Grote,[f] K.G. Gulamov,[b] V.G. Gulyamov,[d] V.K. Gupta,[c] S. Hackel,[h] H.H. Heckman,[i] B. Jakobsson,[j] B. Judek,[k] F.G. Kadyrov,[b] H. Kallies,[h] Y.J. Karant,[i] S.P. Kharlamov,[a] S. Kitroo,[c] J. Kohli,[c] G.L. Koul,[c] V. Kumar,[e] P. Lal,[e] V.G. Larinova,[a] P.J. Lindstrom,[i] L.S. Liu,[g] S. Lokanathan,[e] J. Lord,[f] N.S. Lukicheva,[b] L.K. Mangotra,[c] N.V. Maslennikova,[a] E. Monnand,[l] S. Mookerjee,[e] C. Mueller,[h] S.H. Nasyrov,[d] W.S. Nawotny,[b] G.I. Orlova,[a] I. Otterlund,[j] N.G. Peresadko,[a] S. Persson,[j] N.V. Petrov,[d] R. Raniwala,[e] S. Raniwala,[e] N.K. Rao,[c] J.T. Rhee,[h] N.G. Salmanova,[a] W. Schulz,[h] F. Schussler,[l] V.S. Shukla,[e] D. Skelding,[f] K. Soderstrom,[j] E. Stenlund,[j] R.S. Storey,[k] J.F. Sun,[m] M.I. Tretyakova,[a] T.P. Trofimova,[d] Z.O. Weng,[m] R.J. Wilkes,[f] G.F. Xu,[n] and P.Y. Zheng[n]

a) Lebedev Institute, Moscow, USSR
b) Physical-Technical Institute, Tashkent, USSR
c) University of Jammu, Jammu, India
d) Institute of Nuclear Physics, Tashkent, USSR
e) University of Rajasthan, Jaipur, India
f) University of Washington, Seattle, WA, USA
g) Hua-Zhong Normal University, Wuhan, P.R. China
h) Philipps University, Marburg, Fed. Rep. Germany
i) Lawrence Berkeley Laboratory, Berkeley, CA, USA
j) University of Lund, Lund, Sweden
k) National Research Council, Ottawa, Canada
l) C.E.N., Grenoble, France
m) Shanxi Normal University, Lingfen, P.R. China
n) Academica Sinica, Beijing, P.R. China

ABSTRACT:

The fragmentation of 200A GeV ^{16}O projectiles in nuclear emulsion into projectile fragments of $Z \geq 2$ has been examined in terms of their production rates, charge and multiplicity distributions and their dependence on target-fragment multiplicities. The angular distribution of He (Z=2) projectile fragments is found to be dependent on the He multiplicity. These data, when compared to similar data at 2A GeV, are, within errors of measurement, in accord with energy independence in all aspects, satisfying the condition of limiting fragmentation.

INTRODUCTION:

The acceleration of ^{16}O ions up to 200$\underline{A}$ GeV at CERN and 14.6$\underline{A}$ GeV at Brookhaven heralds a significant advance in the field of relativistic heavy ion physics. In conjunction with the studies of particle production in interactions of ^{16}O with emulsion nuclei at 200$\underline{A}$ GeV by the EMU-01 collaboration for purposes of understanding hadronization in the nuclear environment [1], we have also examined interactions that exhibit the fragmentation of the incident ^{16}O nucleus. In such interactions, projectile fragments are emitted in a small forward angular cone about the direction of the incident ion at near beam velocity. The angular distributions are characteristically gaussian-shaped. Their widths are, to the first approximation, governed by the Fermi motion of the nucleons within the fragmenting nucleus [2,3]. In this work we report on measurements in emulsion chambers and stacks on projectile and target fragmentation, with specific enphasis on the angular distribution of He (Z=2) projectile fragments (PFs) from peripheral 200$\underline{A}$ GeV ^{16}O-Em interactions. These observations are then compared with similar data taken with ^{16}O and ^{12}C beams at 2$\underline{A}$ GeV.

DETECTORS AND MEASURING DEVICES:

In late 1986 fifty emulsion chambers, 10 x 10 x 10 cm^3 in volume, and six emulsion stacks, up to 20 cm in length, were exposed to the CERN SPS ^{16}O beam at energies 60$\underline{A}$ and 200$\underline{A}$ GeV. (For details see Ref. 1 and references therein.)

The measuring systems used in this work incorporate microscopes with digital readout of the xyz state coordinates in 1 μm units (typically). With such systems, emission angles are measured to accuracies $\sigma_\theta \sim 3 \times 10^{-5}$ rad, or, expressed in terms of pseudorapidity $\eta = -\ln(\tan \theta/2)$, $\sigma(\eta) \sim 0.1$-0.2 at $\eta=9$, the pseudorapidity characteristic of He PFs

of ^{16}O at 200A GeV. The measured coordinates of all tracks (including vertex) were measured relative to adjacent, non-interacting beam tracks, and subjected to least squares, 3-dimensional reconstruction programs that yield particle multiplicities, projected and space-angles and pseudorapidity distributions on an event-by-event basis.

SCANNING PROCEDURES:

Conventional "along-the-track" scanning was used to locate ^{16}O-Em interactions in the emulsion stacks. The data sample thereby obtained is virtually bias-free, with the charges of the emitted particles determined by gap-length distributions and/or δ-ray densities. Data recorded for each event pertinent to this work include the multiplicities and emission angles of shower (Z=1) particles and PFs with $Z \geq 2$. In addition, the number of heavily ionizing fragments having grain densities $g \geq 1.4g_{min}$ associated with the target nucleus, denoted by N_h was also recorded for each event.

Events occurring in the emulsion chambers were collected by "area scanning" the normally-incident beam in the 350 μm-thick target plates. Because of the limited volume of emulsion in which an event must be detected, there is an inherent bias against the detection of events that exhibit low shower-particle, projectile-and/or target-fragment multiplicities, i.e., events that are nominally a prerequisite for the presence of peripherally-produced PFs. To minimize this bias, the emulsion chambers were scanned under 22x oil objectives with 10x oculars, which allows one to detect events with shower multiplicities $n_s \leq 10$ and $N_h \leq 1$ with high efficiency. Because PFs cannot be resolved within the target plate, particles emitted within the forward, fragmentation cone (0.20 mrad for PFs with $Z \geq 2$) in each event were examined at distances up to 4 cm from their origin, sufficient to attain complete resolution of the PFs, if present. Too, because of their high rates

of ionization, PFs having $Z \geq 2$ were unambiguously resolved from Z=1 shower particles by inspection.

The identification of Z=2 PFs is unique when the multiplicities of the PFs are 3 and 4. For multiplicities of 2, a visual comparison of the track diameters enabled the observer to determine the (non) equality of the charges of the PFs. PFs of equal charges were deemed to be due to He nuclei, because the production of 2 PFs each with Z=3 or 4 is extremely rare. The smaller of two unequal charges was taken to be due to He. Only for single PF emission was absolute charge estimation necessary. Although visual estimation of track diameters, i.e., charge, was made in each case, our sample of 1He events can reasonably be expected to include some misidentified Z=3, and possibly Z=4, PFs. Estimates of the upper limits of the correction factors can be, and have been, applied to the 1He data to eliminate the effects of background Z=3,4 PFs.

Emulsion chambers and stacks are complementary in this experiment. Specifically, the data collected from stacks are largely unbiased. However, the accuracy in determining the vector direction of particle tracks is degraded by distortions in the emulsion and the need to apply shrinkage-factor corrections to the vertical component of the track vectors. The advantages gained by use of chambers are that angular data are accurate, limited only by the accuracies of the microscope stage coordinates and the geometrical configuration of the chambers. Measurements are simplified and secondary reactions reduced to a minimum because of the low average density of the chamber itself.

RESULTS:

Projectile and Target-Fragment Distributions:

Table I presents the relative rates of production of projectile fragments from ^{16}O-Em interactions in nuclear emulsion at relativistic energies. The data are categorized according to Z_{max}, the maximum charge of the PFs emitted in each event, and, in the case of He, their multiplicities. We observe that PFs with $Z \geq 3$ are often accompanied by He PFs, i.e., by 1He PF in ~ 20%, and by 2He PFs in ~ 2%, of the events of this class. Events grouped under "none" comprise those that involve the emission of Z=1 (shower) particles only, hence can be associated with complete disintegration of the projectile.

As we shall do henceforth, Table I compares the production of PFs from ^{16}O interactions in emulsion at 200A GeV with those observed at 2A GeV [4]. The observations clearly exhibit energy independence, the data agreeing to the extent that the errors associated with the data points overlap in all channels.

In Fig. 1 we interrelate the total charge of PFs ($Z \geq 2$), ΣZ_{PF}, produced in interactions having at least 1He PF, with the associated mean number $\langle N_h \rangle$ of heavily ionizing fragments emitted from the target nucleus. The range of ΣZ_{PF} varies from 2, i.e., where 1He is emitted, to 8, where the total incident charge of the ^{16}O appears in the PFs. The 200A GeV data are plotted as solid points; the 2A GeV data as open points. These data reveal that the degree of target excitation, as represented by $\langle N_h \rangle$, is strongly correlated with the sum of the charges possessed by the PFs. Qualitatively, the greater the fragmentation of the projectile, i.e., the smaller the sum ΣZ_{PF}, the greater is the degree of fragmentation of the target. Specific points of interest are: i) the data exhibit energy independence, although we cannot exclude the possibility for a small systematic difference between the values of $\langle N_h \rangle$ at 2A and 200A GeV. ii) target excitation depends only on

ΣZ_{PF}, irrespective of the distribution of charges that contribute to the particular sum, and iii) $\langle N_h \rangle$ decreases approximately linearly with ΣZ_{PF}. We note that linearity may not be true at low values of ΣZ_{PF} where $\langle N_h \rangle$ exceeds 8, the demarcation point between the major light ($Z \leq 8$) and heavy ($Z \geq 35$) target groups in emulsion, indicative of a change in the effective mass of the target nucleus.

Projectile Fragmentation, Z = 2:

The intrinsic spatial resolution attainable with emulsion chambers/stacks enables us to measure the projected angles θ_x and θ_y, and pseudorapidity of the He PFs associated with the 200A GeV ^{16}O projectile. The angles θ_x and θ_y are the projections of the polar angle of emission of the PFs on the xz and yz planes, where z is the vector direction of the incident ion. Because θ_x and θ_y obey in principle the same physics, they are presented as a single distribution in Fig. 2. The data are based on a total of 97 interactions, giving rise to 178 He PFs with multiplicities $1 \leq N_{He} \leq 3$. No 4-He events were observed in this sample. The angular distribution is gaussian-shaped, with dispersion $\sigma(\theta_{xy}) = (20.5 \pm 1.0) \times 10^{-5}$ rad under the restriction that $|\theta_{xy}| \leq 50 \times 10^{-5}$ rad. Given that the incident momentum is 200A GeV/c, the corresponding (x or y) momentum component is estimated to be $\sigma(p_{xy}) = 155 \pm 8$ MeV/c, taking the average atomic mass of the He PFs to be 3.78. Assuming isotropy in the projectile frame, $\sigma(p_{xy})$ is equivalent to the longitudinal momentum $\sigma(p_z)$, which permits favorable comparisons of this result with $\sigma(p_z) = 137 \pm 2$ MeV/c observed in early experiments on the fragmentation of 2A GeV-^{16}O nuclei [2,5].

Fig. 3 presents the derived momentum dispersions $\sigma(p_{xy})$ of the He PFs as a function of the multiplicity of the He. The closed circles identify the 200A GeV ^{16}O data. These data are to be directly compared with the 2A GeV ^{16}O results plotted as open circles. Also shown in Fig. 3 are (unpublished)

data on the momentum dispersions of 3He and 4He PFs from 2A GeV ^{12}C-CH_2 interactions obtained with the HISS facility [6]. For purposes of comparison, the dispersions are those obtained by fitting all momentum spectra to gaussian distributions for $|p_{xy}| \leq 375$ MeV/c.

The only correction applied to the data shown in Fig. 3 was to the value of $\sigma(p_{xy})$ for the ^{16}O-1He datum of 200A GeV. As commented on above, these data were obtained from emulsion chambers, where the visual inspection of the diameters of the single vertical tracks of PFs was insufficient to resolve Z=2 from Z=3 (and possibly 4). Under the assumptions that i) our 1He data contain a background of events that include all 1Li PFs (unaccompanied by He), ii) given the relative production rates of the 1He and 1Li channels are 13.5 and 3.3%, respectively, [4], and iii) that the momentum dispersion for a PF of mass A_F produced from a beam projectile A_B is $\sigma \propto [x(1-x)]^{1/2}$ where $x = A_F/A_B$, [3], we find that our 1He result should be increased by about 7% to correct for the presence of Li. Similarly, if, as an upper limit, we assume that all 1Be PFs are also included in our sample, then the estimated correction factor increases to about 11%. We have, therefore, applied a +9%(± 2%) correction to our measured value of the momentum dispersion for the 200A GeV 1He channel, a correction equal to about one standard deviation of the experimental uncertainty.

We wish to point out that the 1He, as well as the 2He channel is the composite of all events having 1 (or 2) He PFs, irrespective of the presence of PFs $\geq$ 3. Upon separating the 1He events into those accompanied a) by Z=1 shower particles only and b) by PFs Z$\geq$3, we find that the momentum dispersions of the He PFs are highly dependent on the topologies a) and b). As shown in Fig. 3 for the ^{16}O 1He data at 2A GeV (open circles with dashed error bars), the value of $\sigma(p_{xy})$ for 1He accompanied by Z=1 particles (only) is 22% greater than the composite average of 194 MeV/c, whereas $\sigma(p_{xy})$ for 1He with PFs Z$\geq$3 is 27% less than the composite average. Hence, it is evident that the observed momentum

(angular) distribution of 1He events in a given experiment depends markedly on the relative efficiencies for detecting these classes of 1He events.

Conclusions apparent from Fig. 3 are: i) The dispersions $\sigma(p_{xy})$ of He PFs from ^{16}O at 200A and 2A GeV are in good agreement, indicative of energy independence. ii) This energy independence, i.e., limiting fragmentation, also appears to extend to the individual He-multiplicity channels as well, with the dispersions of the He decreasing with increasing He multiplicity, or alternatively, (see Fig. 1) with decreasing target multiplicity $\langle N_h \rangle$. iii) These general features are also observed in ^{12}C-CH_2 interactions, where the momentum distributions of the 3He and 4He PFs were attained with the HISS facility using magnetic rigidity and particle identification techniques.

At this stage of our investigations, correlations between shower particles and PFs have not been studied. Indeed, the number of shower particles, n_s, produced in events studied here rarely exceeds 50, with an average number in the range of ~ 20 to 25. Such events are characteristic of small nuclear involvement of the projectile.

The presentation of the emission angles of the He PFs in terms of pseudorapidity η, as in Fig. 4, clearly identifies the particles at the highest values of η, e.g. $\eta > 8$, that are observed in the pseudorapidity distributions for low ($n_s < 50$) multiplicity ^{16}O-Em events at 200A GeV as beam-velocity fragments of the incident projectile [1].

The solid curve in Fig. 4 is the predicted η-distribution based on the ^{16}O-He spectrum measured at 2A GeV ($\sigma(p_z) = 137$ MeV/c [2]). The observed value $\langle \eta \rangle = 9.15 \pm 0.06$, with η in the range $7.6 \leq \eta \leq 13$, is in good agreement with the spectrum derived from the transformation of 2A GeV data to 200A GeV.

SUMMARY:

The angular and derived momentum distributions of He PFs we have observed in ^{16}O-Em interactions at 200A GeV are characteristically gaussian - shaped with widths σ that are comparable to those due to Fermi motion in the projectile nucleus. Of particular importance is the result that the "Fermi motion" and the σ of the momentum distribution of He PFs are, in fact, dependent on the multiplicity of the emitted He PFs, decreasing with increasing multiplicity, and, at a given multiplicity, dependent on the presence (or not) of PFs $Z \geq 3$ in final state. This behavior is, within the errors of our measurement, independent of beam energy, and, at 2A GeV, is also exhibited in the He PF spectra from ^{12}C - CH_2 interactions.

As a practical result, this observation extends the validity of the assumption of energy independence of the parameter σ used in the estimation of the primary energies of fragmenting nuclei, e.g., in cosmic rays, from the angular distribution of He PFs --- provided the dependence of the momentum distributions on He PF multiplicities is taken into account.

The general feature of projectile fragmentation in ^{16}O-Em interactions, derived from a comparison of the results of this experiment at 200A GeV with similar data taken at 2A GeV, is that energy independence, i.e. limiting fragmentation, is sustained of the interval $2 \leq E/A \leq 200$ GeV. In addition to the angular dependence of He PFs with the He multiplicity cited above, this energy independence encompasses i) the production rates of PFs, $Z \geq 2$, and ii) the charge and multiplicity distributions and their dependence on target multiplicites, N_h. We find that the associated target-fragment multiplicities decrease monotonically with increasing total charge ΣZ_{PF} of the emitted PFs ($Z \geq 2$). Thus, we deduce that the degrees of excitation energy of the projectile and target nuclei are directly correlated, an effect that is furthermore independent of beam energy.

ACKNOWLEDGMENT:

Kudos to the CERN staff of the PS and SPS for their outstanding performance in producing the ^{16}O beam for this experiment, with special credit to G. Vanderhaeghe, K. Ratz, N. Doble, P. Grafstrom, M. Reinharz, H. Sletten and J. Wotschack. We are grateful for the assistance of A. Oskarsson in monitoring the beam during the exposures of the emulsion, and, most importantly, for the contributions given by the scanning/measuring staffs within the collaboration. The financial support from the Swedish NFR, The German Federal Minister of Research and Technology, and the U.S. Department of Energy under Contract DE-AC03-76SF00098 and NSF in the USA are gratefully acknowledged.

REFERENCES:

[1] EMU-01 collaboration, M.I. Adamovich, et al., Phys. Lett B201 (1988) 397.

[2] D.E. Greiner, P.J. Lindstrom, H.H. Heckman, B. Cork and F.S. Bieser, Phys. Rev. Lett. 35 (1975) 152.

[3] A.S. Goldhaber, Phys. Lett. B53 (1974) 306.

[4] B. Judek, 14th International Cosmic Ray Conference, vol. 7 (1975) 2342. Also private communication (1988).

[5] H.H. Heckman, D.E. Greiner, P.J. Lindstrom, and H. Shwe, Phys. Rev. C17 (1988) 1735.

[6] P.J. Lindstrom, private communication (1988).

Figure Captions:

Fig. 1 Mean number of heavily ionizing target fragments ($g \geq 1.4g_{min}$), N_h, versus ΣZ_{PF}, the total charge of PFs ($Z \geq 2$) emitted in ^{16}O-Em collisions The fragmentation channels are indicated. The closed and open data points identify the 200A GeV and 2A GeV data, respectively.

Fig. 2 Projected polar angles θ_x and θ_y of the projectile fragments for ^{16}O-Em interactions at 200A GeV. The solid curve is the gaussian fit to the data, $|\theta_{xy}| \leq 50 \times 10^{-5}$ rad. The width of the distribution is $\sigma(\theta_{xy}) = (20.5 \pm 1.0) \times 10^{-5}$ rad, corresponding to a momentum $\sigma(p_{xy}) = 155 \pm 8$ MeV/c. The insert figure defines the angles θ_x and θ_y.

Fig. 3 Momentum widths $\sigma(p_{xy})$ versus multiplicity of He PFs from ^{16}O-Em interactions at 200A GeV (closed circles), at 2A GeV (open circles), and from ^{12}C-CH_2 interactions at 2A GeV (open squares). Note the shift in the upper (^{12}C) abscissa. The 2A GeV-^{16}O data for ^{1}He shown with dashed error bars give the momentum widths for ^{1}He PF events with Z=1 particles only (upper value) and for ^{1}He PF events with PFs $3 \leq Z \leq 6$ (lower value).

Fig. 4 Pseudorapidity distribution of He PFs. The smooth curve is the expected distribution extrapolated from 2.1A GeV.

TABLE I Relative production, in percent, of projectile fragments from 200A- and 2A-GeV ^{16}O nuclei in nuclear emulsion. Data are categorized by the maximum charge (and its multiplicity) of the emitted PFs.

Energy (AGeV)	Number of events	Projectile Fragments $Z \geq 2$					
		1He	2He	3He	4He	$Z \geq 3$	None
200	339	15.9±1.8	11.5±1.6	6.2±1.3	0.9±0.5	35.1±2.1	30.4±2.1
2	1192	13.5±0.9	10.2±0.8	6.7±0.7	0.7±0.2	36.6±1.1	32.4±1.1

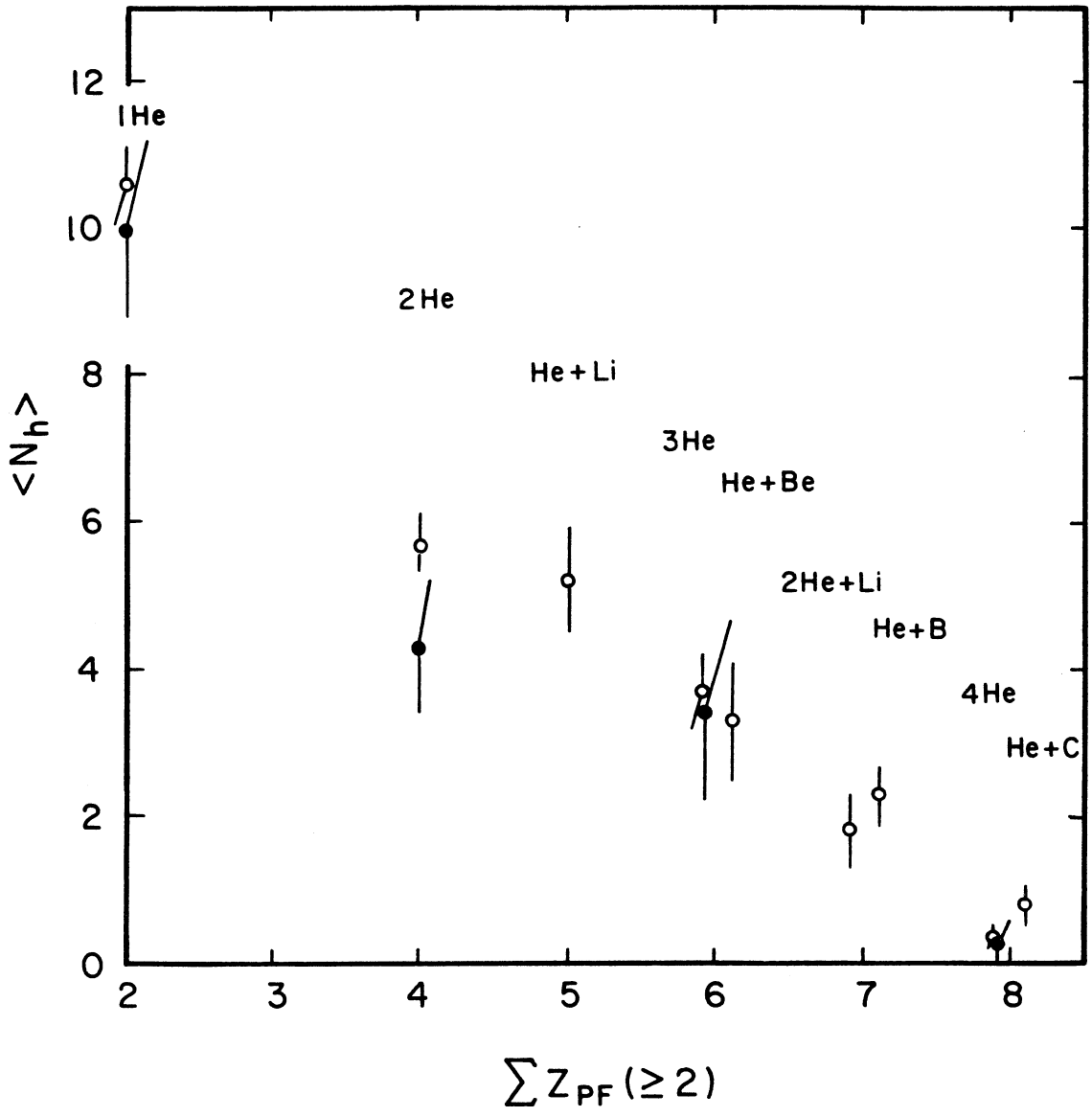

XBL 886-2064

Fig. 1

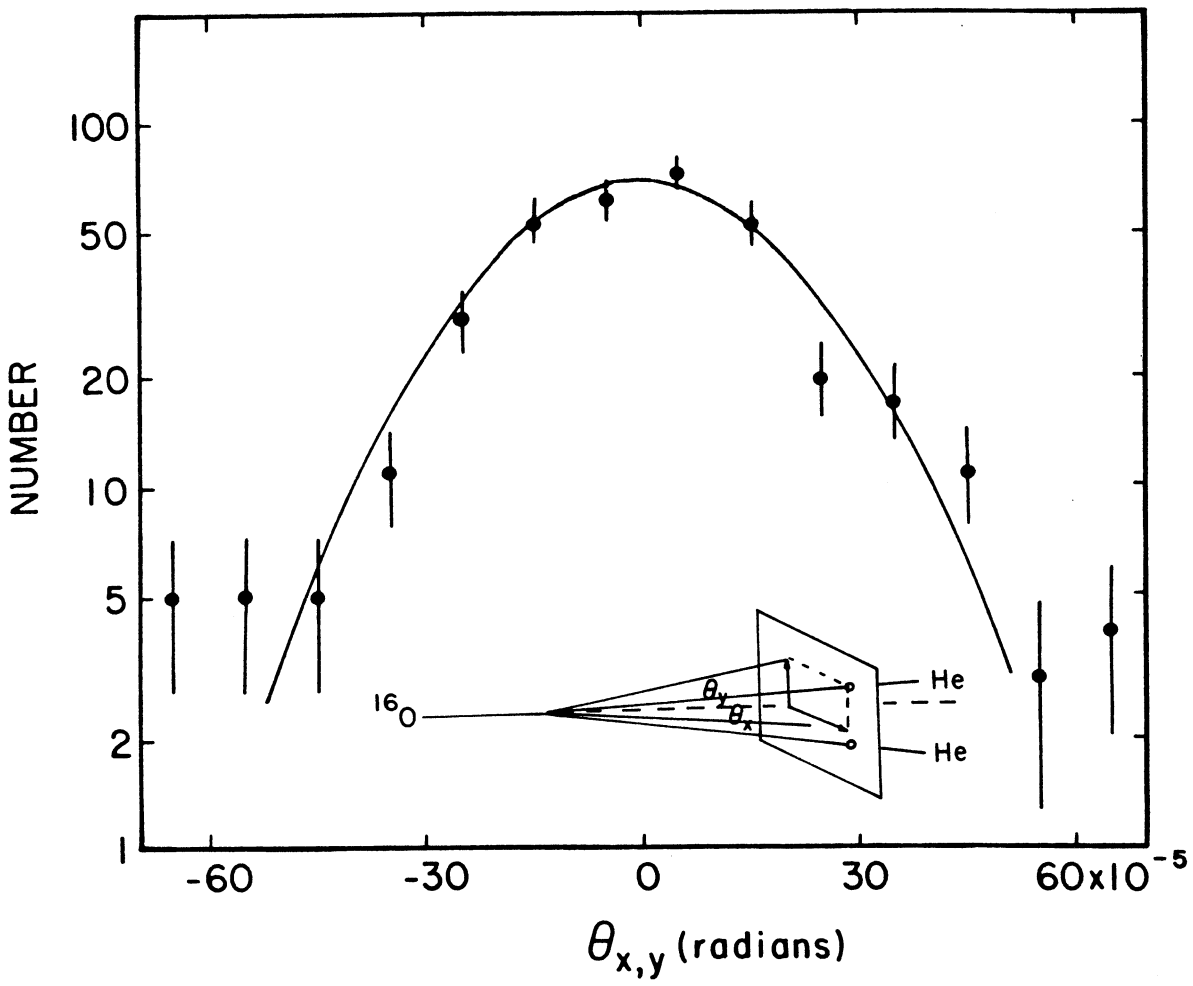
100
50
20
10
5
2
1
NUMBER
-60
-30
0
30
60x10⁻⁵
θx,y (radians)
16O
θy
θx
He
He
XBL 886-2063

Fig. 2

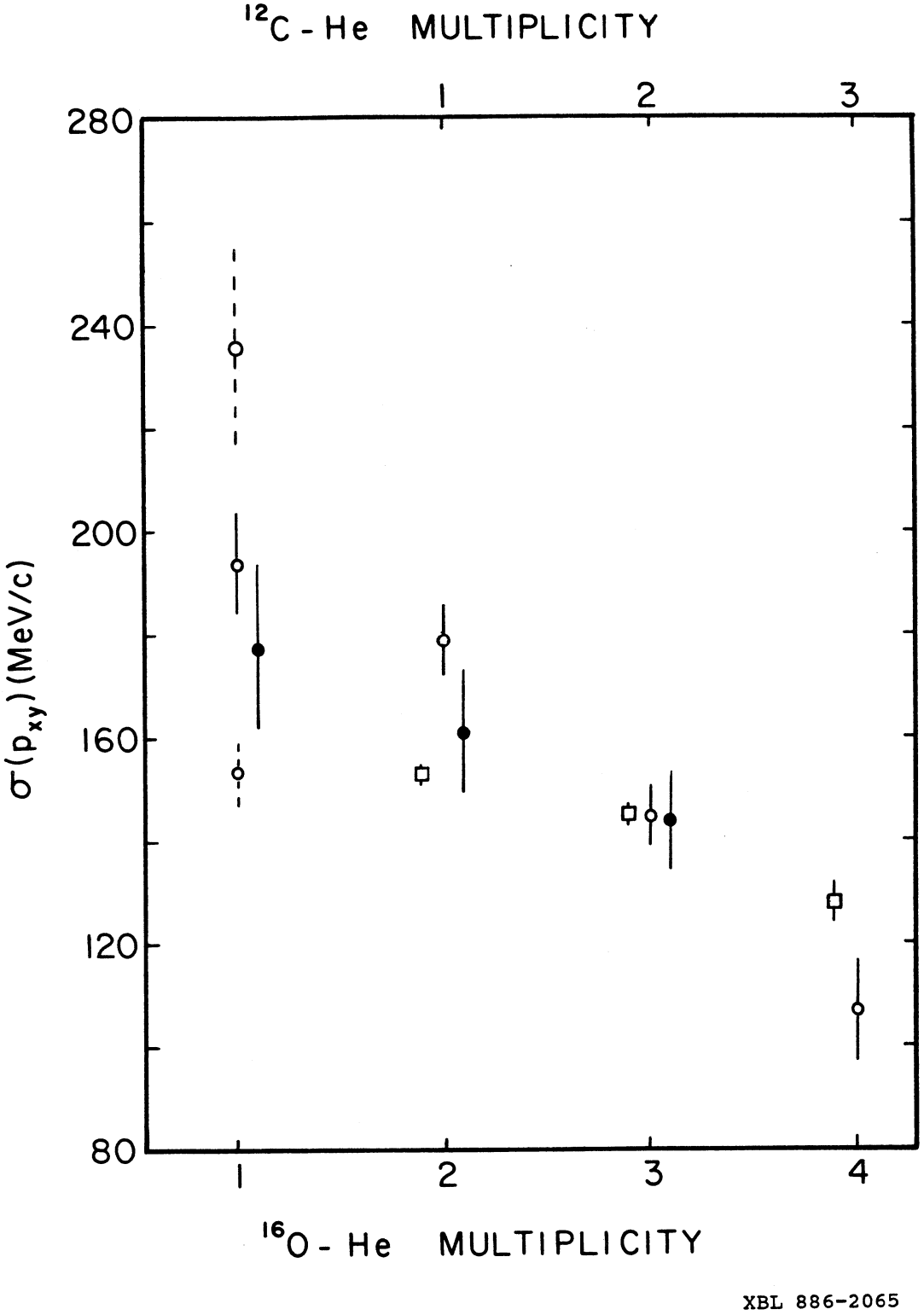
^{12}C - He MULTIPLICITY
1
2
3
280
240
200
160
120
80
$\sigma(p_{xy})$ (MeV/c)
1
2
3
4
^{16}O - He MULTIPLICITY
XBL 886-2065

Fig. 3

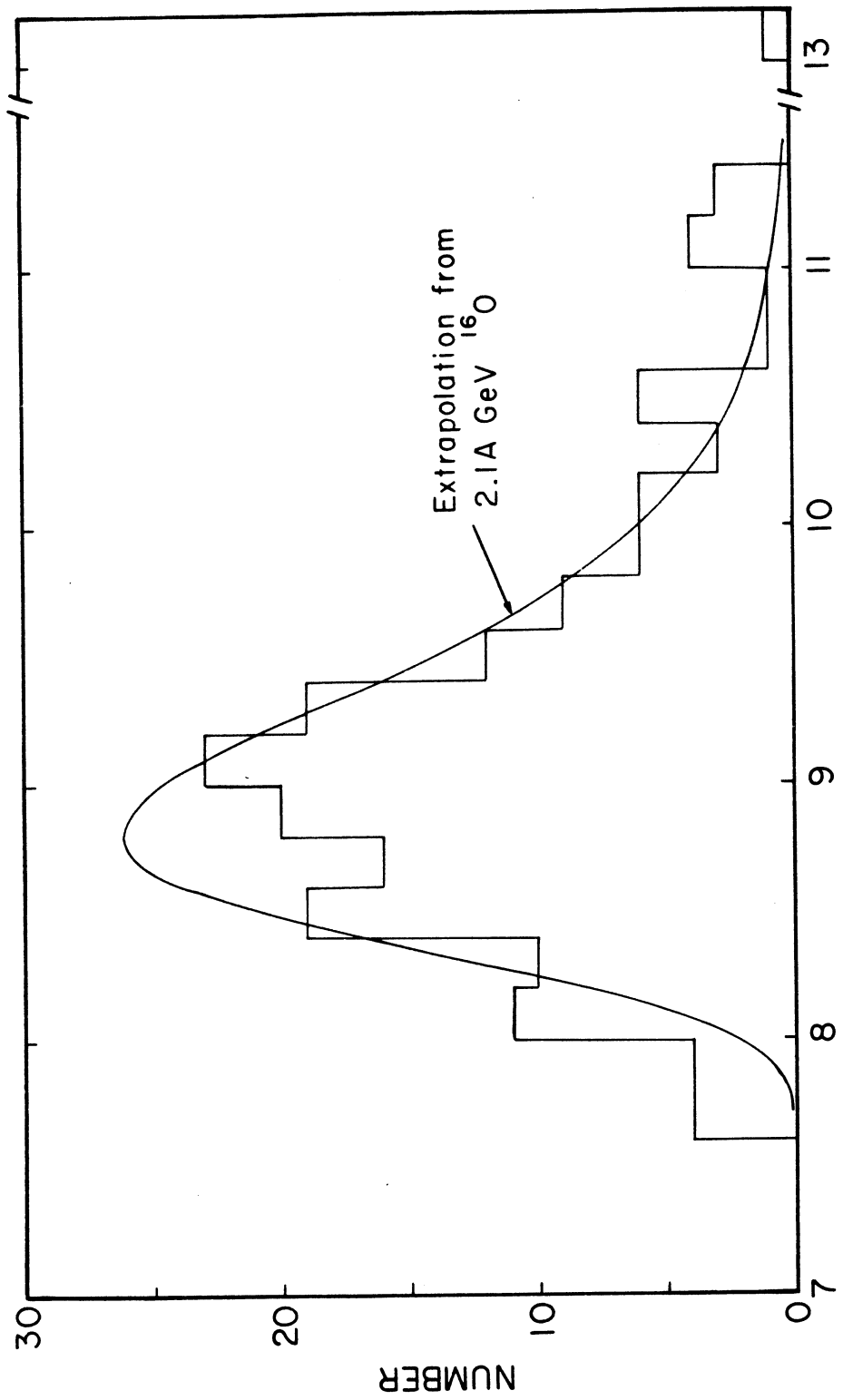

XBL 886-2066

Fig. 4